ARTICLES
PUBLISHED ONLINE: 1 JUNE 2014 | DOI: 10.1038/NPHOTON.2014.114
nature photonics

Emitters of *N*-photon bundles

C. Sánchez Muñoz[1], E. del Valle[1], A. González Tudela[2], K. Müller[3,4], S. Lichtmannecker[3], M. Kaniber[3], C. Tejedor[1], J. J. Finley[3] and F. P. Laussy[1]*

Controlling the output of a light emitter is one of the basic tasks in photonics, with landmarks such as the development of the laser and single-photon sources. The ever growing range of quantum applications is making it increasingly important to diversify the available quantum sources. Here, we propose a cavity quantum electrodynamics scheme to realize emitters that release their energy in groups (or 'bundles') of *N* photons (where *N* is an integer). Close to 100% of two-photon emission and 90% of three-photon emission is shown to be within reach of state-of-the-art samples. The emission can be tuned with the system parameters so that the device behaves as a laser or as an *N*-photon gun. Here, we develop the theoretical formalism to characterize such emitters, with the bundle statistics arising as an extension of the fundamental correlation functions of quantum optics. These emitters will be useful for quantum information processing and for medical applications.

The photon is the building block of light. Every state of the electromagnetic field exists as a superposition of photons, even classical states, which are Poisson distributions. Particular combinations of photons—ranging from more stringent distributions to entangled superpositions—are required to power quantum technology. Cavity quantum electrodynamics (cQED)[1] is one flexible platform used to sculpt desired states of light. These laboratories of the extreme allow the interaction of light with matter to be controlled at the ultimate quantum limit. We show here how they can be used to realize a family of N-photon emitters—sources that release their energy exclusively in groups (or bundles) of N photons (where N is an integer)—in effect providing us with light composed of building blocks that are no longer single photons. This ability to replace the quantum of light with a bundle has unforeseeable consequences, both for applications and for fundamental physics. For instance, it renormalizes the link between the energy of the fundamental unit of excitation to its frequency via a magnified Planck constant, $E = Nh\nu$. The type of emission can be varied with the system parameters to realize both N-photon lasers and photon guns[2] at the N-photon level. Such highly non-classical emitters should find use in the development of new generations of light sources[3,4], the production of NOON states[5], for quantum lithography and metrology[6], and also for medical applications, allowing greater penetration lengths and increased resolution with minimum harm to tissue[7,8]. The recent demonstration that biological photoreceptors are sensitive to photon statistics[9] may also render such sources highly relevant for studies of biological photosystems and, potentially, of quantum biology[10].

Jaynes–Cummings to Mollow dynamics transition

Our scheme relies on the cQED paradigm of one two-level system within a cavity (Fig. 1). This can be realized in a wide range of physical systems, from atoms in optical cavities[11] to superconducting qubits in microwave resonators[12] and quantum dots in microcavities[13]. The dynamics is described by the Jaynes–Cummings Hamiltonian[14] $H_0 = \omega_a a^\dagger a + \omega_\sigma \sigma^\dagger \sigma + g(a^\dagger \sigma + \sigma^\dagger a)$, where a and σ are the second quantization lowering operator of the light field (boson statistics) and the quantum emitter (QE, two-level system), respectively, with corresponding free energies ω_a and ω_σ and coupling strength g. The configuration under study involves the resonant excitation of the QE[15–17] by an external laser, far in the dispersive regime within the cavity $\left(|\omega_a - \omega_\sigma| \gg g\sqrt{N+1}\right)$[18–20]. The energy structure of H_0 is presented in Fig. 2a, with the QE at $\Delta/g = -60$ ($\Delta = \omega_a - \omega_\sigma$), where the states are essentially the bare ones. A laser of frequency ω_L and pumping intensity Ω is included by adding $H_\Omega = \Omega(e^{-i\omega_L t}\sigma^\dagger + e^{i\omega_L t}\sigma)$ to H_0. We assume the rotating wave approximation, the validity of which is justified in Supplementary Section III. At pumping that is low enough not to distort the level structure one can selectively excite a state with N photon(s) in the cavity at the $(N+1)$th rung by adjusting the laser frequency to

$$\omega_N \approx \omega_a + \frac{\sqrt{4(N+1)g^2 + \Delta^2} - \Delta}{2(N+1)} \qquad (1)$$

where $N \in \mathbf{N}$ (ref. 21). This is shown in Fig. 2a for $N = 2$, corresponding to the excitation of the third rung, with a photon blockade[22,23] at all other rungs (above and below)[24,25]. The positions of the resonances are shown in Fig. 3b. In the absence of dissipation, exciting a resonance leads to the generation of an exotic brand of maximally entangled polaritons of the type $(|0g\rangle \pm |Ne\rangle)/\sqrt{2}$ rather than the usual case $(|0e\rangle + |1g\rangle)/\sqrt{2}$. The dynamics of the system for $N = 2$ is presented in Fig. 4a. Strikingly, full-amplitude Rabi oscillations between the $|0g\rangle$ and $|Ne\rangle$ states are observed. Further characterization of these remarkable quantum states is provided in Supplementary Section I. We now consider towards the configuration that will bring such resonances to fruition in terms of applications.

When increasing pumping, resonances in the amplitude of the Rabi oscillations persist, but are blueshifted due to the dressing of the states by the laser. The level structure becomes that of a dressed atom[26] strongly detuned from a cavity mode[27], bridging the Jaynes–Cummings dynamics with another fundamental model of light–matter interaction, namely the Mollow physics of resonance

[1]Condensed Matter Physics Center (IFIMAC), Departamento de Física Teórica de la Materia Condensada, Universidad Autónoma de Madrid, 28049 Madrid, Spain, [2]Max-Planck-Institut für Quantenoptik, Hans-Kopfermann-Strasse 1, 85748 Garching, Germany, [3]Walter Schottky Institut, Technische Universität München, Am Coulombwall 4, 85748 Garching, Germany, [4]E. L. Ginzton Laboratory, Stanford University, Stanford, California 94305, USA.
*e-mail: fabrice.laussy@gmail.com

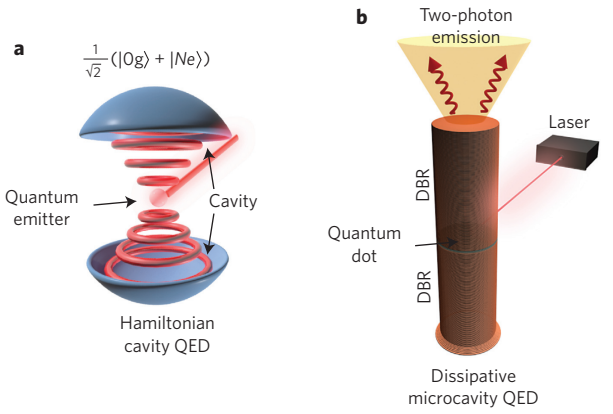

Figure 1 | Hamiltonian and dissipative cavity QED. a, cQED brings QED (the theory of light–matter interactions) under prolonged scrutiny at the level of a few photons and in the presence of a quantum emitter. An external laser can be applied to the emitter to drive its dynamics. We show how peculiar quantum superpositions can be realized and the emission subsequently forced to take place exclusively in bundles of N photons. **b**, A possible solid-state implementation of our proposal places a quantum dot in a micropillar. With excitation from the side with a conventional laser, one can collect, in the cavity, emission as the output from a quantum laser or a quantum gun, depending on the system parameters. DBR, distributed Bragg reflector.

fluorescence[28]. The strong coupling that was previously dominated by the interaction between the QE and a cavity photon and was probed by the laser is now dominated by the interaction of the QE with the laser photons and is probed by the cavity. This elegant transition between the two pillars of nonlinear quantum optics brings the resonances in equation (1) to the form

$$\omega_N(\Omega) \approx \omega_a + \frac{\sqrt{4(N^2-1)\Omega^2 + N^2\Delta^2} + \Delta}{N^2-1} \qquad (2)$$

Equation (2) is realized when the energy of N cavity photons matches the N-photon transition between the $|-\rangle$ and $|+\rangle$ levels of the dressed atom[29], as shown in Fig. 2b for $N=2$. In the indeterminate case $N=1$, equation (2) should be taken in the limit $N \to 1$, yielding $\omega_L = \omega_a - (2\Omega^2 + \Delta^2/2)/\Delta$ (in the dispersive regime, $\Delta \neq 0$).

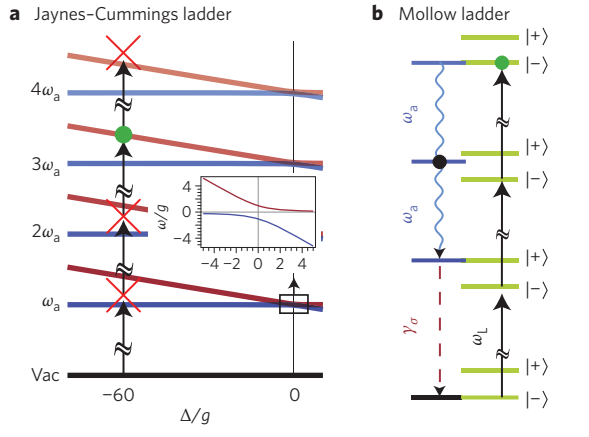

Figure 2 | Energy levels of the two limiting cases of excitation. a, In the low-excitation regime the Jaynes–Cummings ladder (anticrossing magnified in the inset) is probed by resonantly exciting a given rung of the ladder, with photon blockade at all others. **b**, In the high-excitation regime, the laser dresses the QE while the cavity Purcell-enhances an N-photon transition from $|-\rangle$ to $|+\rangle$ (here for $N=2$). A subsequent emission from the QE brings the system back to a $|-\rangle$ state.

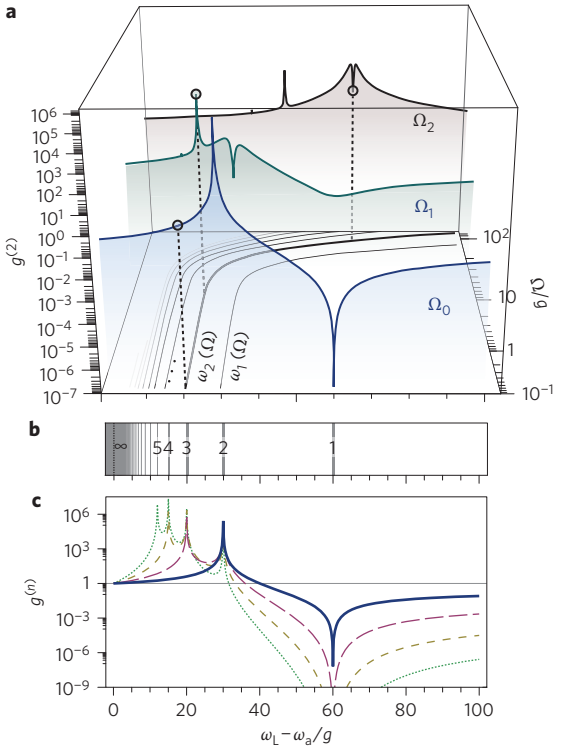

Figure 3 | Resonances in the photon-correlation functions. a, $g^{(2)}$ as a function of ω_L for pumping $\Omega_0 \approx 10^{-2}g$, $\Omega_1 \approx 4g$ and $\Omega_2 \approx 32g$. The resonances $\omega_N(\Omega)$ are shown in the plane (ω_L,Ω). Open circles are the projection of ω_2 on $g^{(2)}$. **b**, Resonant energies to excite the nth rung of the ladder. **c**, $g^{(n)}$ for $n=2$ (solid), 3 (long dash), 4 (short dash) and 5 (dotted) at vanishing pumping with n–1 bunching resonances matching those in **b**. $\Delta/g = -60$ in all panels.

All the dynamics discussed so far correspond to systems that are Hamiltonian in nature, such as atomic cQED realizations[30].

Dissipation as a trigger of quantum emission

Strong dissipation, as in semiconductor cQED, is not always detrimental to quantum effects[31,32]. Indeed, Purcell enhancement of the Hamiltonian resonances just described may give rise to giant photon correlations in the statistics of the field detected outside the cavity, instead of Rabi oscillations[33,34]. The corresponding zero-delay photon correlations[35] $g^{(n)} = \langle a^{\dagger n} a^n \rangle / \langle a^\dagger a \rangle^n$ are shown in the limit of vanishing pumping in Fig. 3c. An antibunching dip is observed for each $g^{(n)}$ when resonantly exciting the emitter, followed by a series of $n-1$ huge bunching peaks that match the resonances in equation (1), as plotted in Fig. 3b. In these calculations, the Hamiltonian has been supplemented with superoperators in the Lindblad form to describe dissipation of the cavity (respectively QE) at a rate γ_a (respectively γ_σ)[36] (see Methods). The parameters used are $\gamma_a/g = 0.1$ and $\gamma_\sigma/g = 0.01$. Details of the formalism, as well as its extension to describe decoherence, are given in Supplementary Section VI. As pumping is increased, resonances in $g^{(n)}$ shift along the curves $\omega_N(\Omega)$ in the (ω_L, Ω) space defined by equation (2). This is shown for $g^{(2)}$ in Fig. 3a for three values of pumping (for an animation see the Supplementary Movie), starting with $\Omega_0 = 10^{-1}g$, close to the vanishing pumping case shown in Fig. 3c. Following $g^{(2)}$ along the ω_2 resonance reveals that a new peak emerges out of a uniform background, reaching a maximum $g^{(2)} \approx 3{,}649$ at the pumping $\Omega_1 \approx 4g$ (middle trace) before a depletion of the resonance forms for higher pumping, reaching its minimum along ω_2 of $g^{(2)} \approx 17$ at $\Omega_2 \approx 32g$ (background trace). So far, we have therefore transferred some

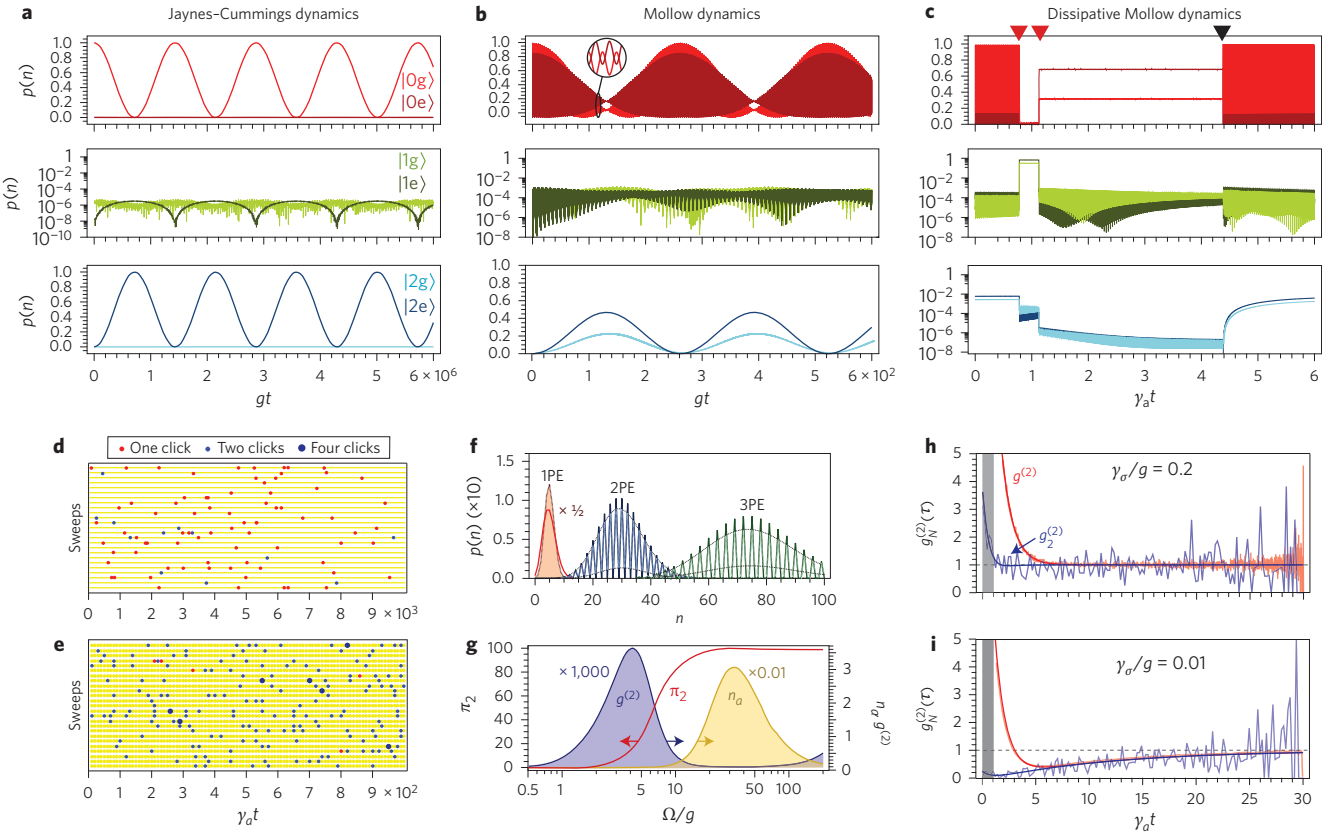

Figure 4 | Dynamics of the emission when probing the two-photon resonance in various regimes of excitation. a, Wavefunction evolution at the two-photon resonance pictured through the probability of the system to be in any of the states $|ng/e\rangle$. Hamiltonian evolution in the Jaynes–Cummings regime (low pumping). **b**, Hamiltonian evolution in the Mollow regime (high pumping). **c**, Quantum trajectory during two-photon emission in the same regime as in **b**, but in the presence of dissipation. **d**,**e**, Cavity-photon clicks as they would be recorded by a streak camera (25 sweeps shown) for pumping values Ω_1 (**d**) and Ω_2 (**e**) at $\omega_2(\Omega)$. In **d**, the emission is highly bunched, although it largely consists of single clicks ($g^{(2)} = 3{,}649$ and $\pi_2 = 16\%$). In **e**, $g^{(2)} = 17$ with $\pi_2 = 98.8\%$. **f**, Ideal *N*PE (*N*-photon emission) in thick lines and 99% *N*PE in translucent lines with an envelope to guide the eye. **g**, Pumping dependence of π_2 (left axis) and $g^{(2)}$ (right axis) (from 0 to 3,649) and n_a (from 0 to 0.03) following $\omega_2(\Omega)$. **h**,**i**, Second-order photon correlations at the $N = 1$ (red) and $N = 2$ (blue) level, from equation (6) (smooth curve) and from Monte Carlo clicks (data).

attributes of the remarkable quantum states produced by the cQED system to the outside world. We now proceed to show in which regimes and in which sense this transfer can actually be used for applications.

Strong correlations do not guarantee useful emission

The resonances in $g^{(n)}$ are indicative of strong correlations, but not in an intuitive way nor in a particularly useful one for applications. Indeed, $g^{(2)}$ (we discuss the case $n = 2$ with no loss of generality) is unbounded and cannot be interpreted in terms of the probability of two-photon emission. Other quantities to measure correlations, such as the differential correlation function[37] or the surge[38], present the same problem. To gain insights into the dissipative context, we turn to a quantum Monte Carlo approach[39], where one follows individual trajectories of the system and records photon clicks whenever the system undergoes a quantum jump. A tiny fraction of such a trajectory is presented in Fig. 4c (a larger fraction is provided in Supplementary Section II). This shows the probabilities of the system to be in the states $|ng/e\rangle$ for n up to 2 (probabilities in higher rungs are included in the numerical simulation).

Until time $t \approx 0.8$ (in units of $1/\gamma_a$), the QE essentially undergoes fast Rabi flopping (in an empty cavity) under the action of the laser, corresponding to the Mollow regime. At the same time, the driving of the third rung makes the probability of having two photons in the cavity sizable, as seen in the bottom panel of Fig. 4c, where the combined probability reaches over 1% (while the probability of having one photon is more than one order of magnitude smaller). This relatively high probability of the two-photon state, given the time available to realize it, eventually results in its occurrence. This causes the emission of a first cavity photon (indicated by a red triangle at the top of the figure) that collapses the wavefunction into the one-photon state, which is now the state with almost unit probability. The system is now expected to emit a second photon within the cavity lifetime (second red triangle in Fig. 4c). There is a jitter in the emission of the two-photon state due to the cavity, but this does not destroy their correlation. After the two-photon emission the system is left in a vacuum state but without Rabi flopping; this is restored after a direct emission from the QE (black triangle) and a two-photon state is again constructed, preparing for the next emission of a correlated photon pair. The system is then brought back to its starting point. Although one photon coming from the QE decay is emitted per two-photon emission cycle, it is at another frequency and with a different solid angle. The two-photon emission takes place through the cavity mode and is therefore unspoiled and strongly focused.

Figure 4d,e presents a series of detection events (such as would be recorded by a streak camera photodetector[40]) for the pumping values Ω_1 and Ω_2 of Fig. 3a at $\omega_2(\Omega)$. The horizontal axis represents time, and each point denotes a detection event as the detection spot is raster-scanned across the image. The strong bunching at Ω_1 in Fig. 3a conveys that the number of correlated two-photon events (blue points) in Fig. 4d is much larger than would be expected for

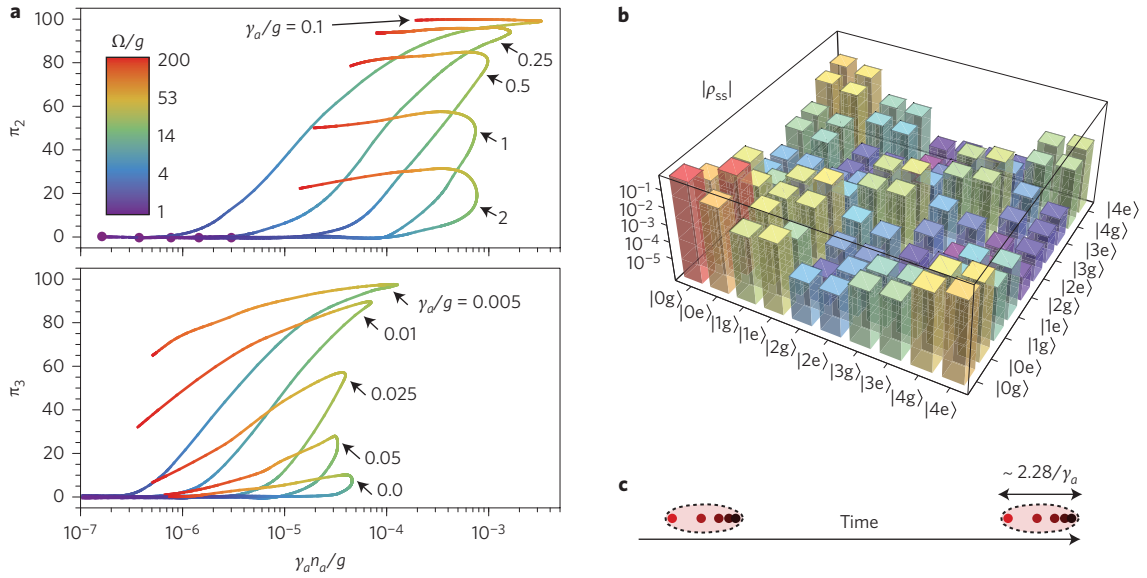

Figure 5 | Efficiency and characterization of *N*-photon emission for $2 \leq N \leq 5$ a, Figures of merit for two- and three-photon emission in the space of purity/emission intensity. Almost pure two- and three-photon emission can be achieved with state-of-the-art cQED samples: $\gamma_a/g = 0.01$ for π_2 and 0.001 for π_3. **b**, Full density matrix of the system in the regime of four-photon emission, showing the predominance of the vacuum and the strong coherence between the 2×2 sub-blocks of 0 and 4 photons and the $1/n$ cascade along the diagonal. **c**, Sketch of two five-photon bundles. Each bundle is composed of photons that pile up together ahead in time due to the mechanism of their production. This structure is not described by the state $|5\rangle$.

a coherent source. Nevertheless, the emission remains predominantly in terms of single photons (red points). Accordingly, although the resonances in the statistics are strong, they are not meaningful for applications. On the other hand, at Ω_2, when the $g^{(2)}$ resonance is depleted, the emission now consists almost exclusively of correlated photon pairs, as can be seen by the dominance of blue points in Fig. 4e.

Definition of purity of *N*-photon emission

Because the standard correlation functions $g^{(n)}$ do not correspond to actual N-photon emission, the problem arises of how to describe what is in fact the most important feature of such an emitter: the amount of N-photon emission. Photon counting[41–43] is a convenient way to do this in practical terms, as an ideal N-photon emitter never produces a number of photons that is not a multiple of N (ref. 44). We observe that for time windows T larger than the coherence time, counting of the photon bundles becomes Poisson distributed, as short time correlations are lost[45]. This distribution is shown in Fig. 4f for the cases of ideal two-photon (2PE) and three-photon (3PE) emission. However, a non-ideal N-photon emitter occasionally emits single photons that spoil these distributions. If bundle events are represented by the Poisson parameter λ_N and single events by λ_1, one finds (see Methods) that the distribution of counting n photons in time window T is given by

$$P_N(n) = e^{-(\lambda_1+\lambda_N)T} \sum_{k=0}^{n} \frac{n!(\lambda_1 T)^{n-Nk}(\lambda_N T)^k}{k!(n-Nk)!} \qquad (3)$$

When the suppression of photon emission that is not a multiple of N is efficient, these parameters are related to the cavity population n_a through $\lambda_N = \gamma_a n_a/N$. As the λ parameters are independent of the time window T, we can define the 'purity' of the N-photon emission π_N as

$$\pi_N = \lambda_N/(\lambda_1 + \lambda_N) \qquad (4)$$

This ratio represents the percentage of the emission that exists as N-photon bundles, which can now be contrasted with $g^{(N)}$, as shown in Fig. 4g for $N = 2$. Here we find the remarkable result that $g^{(2)}$, often described as the probability for two-photon emission, is in fact anticorrelated with π_2, the actual such probability: when $g^{(2)}$ reaches its maximum π_2 is starting to grow, and when π_2 is maximum $g^{(2)}$ is locally minimum, although still larger than one.

We characterize the efficiency of N-photon emission by plotting the purity and emission intensity together (Fig. 5a) for π_2 and π_3. Because N-photon emission is a $(N+1)$th-order process, it is more easily overcome by dissipation as N increases. Nevertheless, almost pure two-photon and three-photon emission is already feasible with state-of-the-art cQED systems. Indeed, ~85% of two-photon emission can already be obtained with current semiconductor samples ($\gamma_a/g \approx 0.5$, $g \approx 12$ GHz)[46,47] with a rate of over 1×10^7 counts per second, while circuit QED systems ($\gamma_a/g \approx 0.01$, $g \approx 50$ MHz)[48] can even reach ~90% of three-photon emission with a rate of 1×10^3 counts per second. N-photon emission takes place when the coupling is large enough for the cavity to stop acting as a mere filter and actually Purcell-enhance the corresponding multiphoton transitions[49]. These results are extremely robust against dephasing, thanks to the short time window in which a bundle is generated and emitted, as is shown in Supplementary Section VI.

Relation between the bundle and a Fock state

We have described the emission of our system in terms of bundles of photons, introducing a terminology that needs to be justified. In quantum theory, a state of the field with exactly N quanta of excitation is a Fock state $|N\rangle$, and it is natural to question whether our device is not precisely an 'emitter of Fock states $|N\rangle$'.

There are subtle links and departures between the two concepts. The Fock state $|N\rangle$ is a well-defined state that can be prepared and maintained exactly. It has no further structure and each of the N photons that compose it is fully indistinguishable from the others. The bundle, on the other hand, arises in a dynamical process of emission, describing the energy released from the cQED set-up to the outside world. The cavity itself is not in the Fock state $|N\rangle$ being, to begin with, in the vacuum most of the time; only in very short temporal windows does it undergo a cascade that sees the field transit through the various Fock states $|n\rangle$ in rapid succession, where $0 \leq n \leq N$ and for a time $1/(\gamma_a n)$ in each of them. Because the

system has a small probability of being in state $|N\rangle$ before the emission and a probability close to one of transiting through each of the intermediate states during the cascade, one obtains the steady-state probability

$$p(n) = \frac{n_a}{N}\frac{1}{n}, \quad \text{for } 1 \le n \le N \tag{5}$$

A snapshot of the full density matrix in the regime of four-photon emission is given in Fig. 5b. This shows the breakdown of the matrix into clusters of 2×2 blocks corresponding to the subspaces of the QE with n photons. The vacuum largely predominates (probabilities are shown in a logarithmic scale), followed by the blocks on the diagonal, which provide $p(n)$ as given by equation (5), and blocks of coherence between the various manifolds, which are small although non-zero, except the coherence elements $|0\mu\rangle\langle 4\nu|$ with $\mu,\nu \in \{g, e\}$, which are large. This confirms the direct manifestation, also in the dissipative regime, of the quantum superposition of the type $(|0g\rangle \pm |Ne\rangle)/\sqrt{2}$.

There remains a trace of this intracavity dynamics in the photodetection. The bundles are strongly correlated in two senses: (1) extrinsically, the emission occurs in groups of N photons, suppressing the release of packets with other numbers of photons; (2) intrinsically, with different time intervals separating successive photons, the first photon is more closely followed by the second one than the second is by the third, and so on until the last photon, which comes within $1/\gamma_a$ of the penultimate photon (Fig. 5c). Clearly, the bundle is a strongly correlated group of closely spaced photons and has a structure that is not described by the abstract object $|N\rangle$ alone. However, regardless of the internal structure of the bundle, it would appear as a Fock state in a measurement integrated over a small time window. Further discussion with the Wigner function can be found in Supplementary Section IV.

Regimes of *N*-photon emission: guns and lasers

Now that we have engineered N-photon emitters we have to ask the same questions as put by Glauber[35] at the dawn of quantum optics regarding the nature of quantum optical coherence for these sources. The answer is as simple as it is beautiful: N-photon emitters are the exact counterpart of conventional emitters, but the unit of emission—the photon—is replaced by a bundle of N photons. We now show that our class of emitters can operate in the same regimes as lasers or photon guns, but with bundles. To do so, we describe the statistics of the bundles when considered as single entities by introducing the generalized correlation functions $g_N^{(n)}$:

$$g_N^{(n)}(t_1, \ldots, t_n) = \frac{\langle \mathcal{T}_-\{\prod_{i=1}^n a^{\dagger N}(t_i)\}\mathcal{T}_+\{\prod_{i=1}^n a^N(t_i)\}\rangle}{\prod_{i=1}^n \langle a^{\dagger N}a^N\rangle(t_i)} \tag{6}$$

where $\mathcal{T}_\pm$ represents the time ordering operators. This upgrades the concept of the nth-order correlation function for isolated photons to bundles of N photons. The case $N = 1$ recovers the definition of the standard $g^{(n)}$, but for $N \ge 2$, normalization to the bundle density makes equation (6) essentially different from the standard correlation functions $g^{(n\times N)}$. Similarly to the single-photon case, the two-bundle statistics

$$g_N^{(2)}(\tau) = \frac{\langle a^{\dagger N}(0)a^{\dagger N}(\tau)a^N(\tau)a^N(0)\rangle}{\langle (a^{\dagger N}a^N)(0)\rangle\langle (a^{\dagger N}a^N)(\tau)\rangle} \tag{7}$$

is the most important. The validity of this definition for $g_2^{(2)}$ is confirmed in Fig. 4h,i, where it is plotted (smooth curve) together with direct coincidences between clicks from the Monte Carlo simulation (data). Such $g_2^{(2)}$ correlations can be measured directly thanks to recent developments in two-photon detection[50]. For the Monte Carlo computation, all events are considered as single photons for the standard $g^{(2)}$ calculation (red curve in Fig. 4h,i), and only two-photon events are considered as the basic unit of emission for $g_2^{(2)}$ (blue curve). Except in the small jitter window of width $1/\gamma_a$ in which they cannot be defined, photon pairs exhibit anti-bunching for long-lived QE, while they are Poisson-distributed for short-lived QE. In the latter case one can check that $g_2^{(3)}(\tau_1, \tau_2) = 1$ except for in the aforementioned jitter window (see Supplementary Section V). The emitter therefore behaves respectively as a two-photon gun and—according to Glauber[35]—as a laser, but at the two-photon level. The effect the QE lifetime has on the statistics of the bundles can be understood as a consequence of the key role the QE emission plays to restore the construction of an N-photon state. At the single-photon level, the standard $g^{(2)}(\tau)$ fails to capture this fundamental dynamics of emission. All this confirms the emergence of a new physics at the two-photon level. The same behaviours hold for higher N.

Methods

System dynamics. To describe dissipation in addition to the Hamiltonian dynamics, we resort to a master equation in the Lindblad form[36]:

$$\dot{\rho} = -i[H, \rho] + \left[\frac{\gamma_a}{2}\mathcal{L}_a + \frac{\gamma_\sigma}{2}\mathcal{L}_\sigma\right]\rho \tag{8}$$

expressed in terms of the Liouvillian super-operator $\mathcal{L}_c\rho = 2c\rho c^\dagger - c^{\dagger A}c\rho - \rho c^\dagger c$, where γ_a and γ_σ are the decay rates of the cavity and quantum emitter, respectively and $H = H_0 + H_\Omega$. By arranging the elements of the density matrix in a vectorial form, we can express this equation as $\dot{\vec{\rho}} = M\vec{\rho}$, from which the steady-state density matrix $\vec{\rho}_{ss}$ is obtained as the null space of the matrix M. A more general expression that takes into account additional dephasing terms is provided and investigated in Supplementary Section VI.

For photon-counting calculations, we solve the same problem using the Monte Carlo method of quantum trajectories, which allows the use of a wavefunction picture in a dissipative context. In this approach, one uses an evolution operator constructed with a non-Hermitian Hamiltonian $H_{\text{eff}} = H - i\frac{\gamma_a}{2}a^\dagger a - i\frac{\gamma_\sigma}{2}\sigma^\dagger\sigma$, whose resulting dynamics can be interrupted in each time step δt by a quantum jump acting on the wavefunction as $c|\psi\rangle/\langle\psi|c^\dagger c|\psi\rangle$ ($c \in \{a, \sigma\}$) with probability $p_c = \delta t\ \gamma_c \langle\psi|c^\dagger c|\psi\rangle$. These jump events are then recorded as photon emissions coming from the cavity or the QE.

Photon-counting distribution for the imperfect *N*-photon emitter. In the limit in which the counting of N-photon bundles becomes Poisson distributed, the random variable X_N that counts them in a time window T follows the distribution $P(X_N = k) = \exp(-\lambda_N T)(\lambda_N T)^{k/N}/(k/N)!$ if k is a multiple of N and is zero otherwise, with a generating function $\Pi_{X_N}(s) = \langle s^{X_N}\rangle = e^{-\lambda_N(1-s^N)}$. A non-ideal N-photon emitter also emits single photons that spoil these distributions. Photon counting then results from the sum of two random variables $X_1 + X_N$, where X_1 is a conventional Poisson process. The generating function of the imperfect N-photon emitter is $\Pi_{X_1+X_N} = \Pi_{X_1}\Pi_{X_N}$, where $\Pi_1 = e^{-\lambda_1(1-s)}$ is the generating function of a Poissonian distribution. The closed-form expression provided in the text is straightforwardly derived as $P_N(n) = \frac{1}{n!}\partial^n\Pi_{X_1+X_N}/\partial s^n|_{s=0}$.

Received 20 December 2013; accepted 23 April 2014; published online 1 June 2014

References

1. Haroche, S. Nobel lecture: Controlling photons in a box and exploring the quantum to classical boundary. *Rev. Mod. Phys.* **85,** 1083–1102 (2013).
2. Lounis, B. & Orrit, M. *Rep. Prog. Phys.* **68,** 1129 (2005).
3. Walther, H., Varcoe, B. T. H., Englert, B.-G. & Becker, T. Cavity quantum electrodynamics. *Rep. Prog. Phys.* **69,** 1325–1382 (2006).
4. O'Brien, J. L., Furusawa, A. & Vučkovic, J. Photonic quantum technologies. *Nature Photon.* **3,** 687–695 (2009).
5. Afek, I., Ambar, O. & Silberberg, Y. High-NOON states by mixing quantum and classical light. *Science* **328,** 879–881 (2010).
6. Giovannetti, V., Lloyd, S. & Maccone, L. Quantum-enhanced measurements: beating the standard quantum limit. *Science* **306,** 1330–1336 (2004).
7. Denk, W., Strickler, J. H. & Webb, W. W. Two-photon laser scanning fluorescence microscopy. *Science* **248,** 73–76 (1990).
8. Horton, N. *et al. In vivo* three-photon microscopy of subcortical structures within an intact mouse brain. *Nature Photon.* **7,** 205–209 (2013).
9. Sim, N., Cheng, M. F., Bessarab, D., Jones, C. M. & Krivitsky, L. A. Measurement of photon statistics with live photoreceptor cells. *Phys. Rev. Lett.* **109,** 113601 (2012).

10. Ball, P. Physics of life: the dawn of quantum biology. *Nature* **474,** 272–274 (2011).
11. Brune, M. *et al.* Quantum Rabi oscillation: a direct test of field quantization in a cavity. *Phys. Rev. Lett.* **76,** 1800–1803 (1996).
12. Fink, J. M. *et al.* Climbing the Jaynes–Cummings ladder and observing its $\sqrt{n}$ nonlinearity in a cavity QED system. *Nature* **454,** 315–318 (2008).
13. Kasprzak, J. *et al.* Up on the Jaynes–Cummings ladder of a quantum-dot/microcavity system. *Nature Mater.* **9,** 304–308 (2010).
14. Jaynes, E. T. & Cummings, F. W. Comparison of quantum and semiclassical radiation theory with application to the beam maser. *Proc. IEEE* **51,** 89–109 (1963).
15. Nguyen, H. S. *et al.* Ultra-coherent single photon source. *Appl. Phys. Lett.* **99,** 261904 (2011).
16. Matthiesen, C., Vamivakas, A. N. & Atatüre, M. Subnatural linewidth single photons from a quantum dot. *Phys. Rev. Lett.* **108,** 093602 (2012).
17. Jayakumar, H. *et al.* Deterministic photon pairs and coherent optical control of a single quantum dot. *Phys. Rev. Lett.* **110,** 135505 (2013).
18. Majumdar, A. *et al.* Linewidth broadening of a quantum dot coupled to an off-resonant cavity. *Phys. Rev. B* **82,** 045306 (2010).
19. Hughes, S. & Carmichael, H. J. Stationary inversion of a two level system coupled to an off-resonant cavity with strong dissipation. *Phys. Rev. Lett.* **107,** 193601 (2011).
20. Laussy, F. P., del Valle, E., Schrapp, M., Laucht, A. & Finley, J. J. Climbing the Jaynes–Cummings ladder by photon counting. *J. Nanophoton.* **6,** 061803 (2012).
21. Chough, Y.-T., Moon, H.-J., Nha, H. & An, K. Single-atom laser based on multiphoton resonances at far-off resonance in the Jaynes–Cummings ladder. *Phys. Rev. A* **63,** 013804 (2000).
22. Birnbaum, K. *et al.* Photon blockade in an optical cavity with one trapped atom. *Nature* **436,** 87–90 (2005).
23. Faraon, A. *et al.* Coherent generation of non-classical light on a chip via photon-induced tunnelling and blockade. *Nature Phys.* **4,** 859–863 (2008).
24. Schuster, I. *et al.* Nonlinear spectroscopy of photons bound to one atom. *Nature Phys.* **4,** 382–385 (2008).
25. Bishop, L. S. *et al.* Nonlinear response of the vacuum Rabi resonance. *Nature Phys.* **5,** 105–109 (2009).
26. Cohen-Tannoudji, C. & Reynaud, S. Dressed-atom description of resonance fluorescence and absorption spectra of a multi-level atom in an intense laser beam. *J. Phys. B* **10,** 345–363 (1977).
27. Zakrzewski, J., Lewenstein, M. & Mossberg, T. W. Theory of dressed-state lasers. I. Effective Hamiltonians and stability properties. *Phys. Rev. A* **44,** 7717–7731 (1991).
28. Mollow, B. R. Power spectrum of light scattered by two-level systems. *Phys. Rev.* **188,** 1969–1975 (1969).
29. Gonzalez-Tudela, A., Laussy, F. P., Tejedor, C., Hartmann, M. J. & del Valle, E. Two-photon spectra of quantum emitters. *New J. Phys.* **15,** 033036 (2013).
30. Gleyzes, S. *et al.* Quantum jumps of light recording the birth and death of a photon in a cavity. *Nature* **446,** 297–300 (2007).
31. Volz, T. *et al.* Ultrafast all-optical switching by single photons. *Nature Photon.* **6,** 605–609 (2012).
32. Majumdar, A., Englund, D., Bajcsy, M. & Vučković, J. Nonlinear temporal dynamics of a strongly coupled quantum-dot–cavity system. *Phys. Rev. A* **85,** 033802 (2012).
33. Del Valle, E., Gonzalez-Tudela, A., Cancellieri, E., Laussy, F. P. & Tejedor, C. Generation of a two-photon state from a quantum dot in a microcavity. *New J. Phys.* **13,** 113014 (2011).
34. Zubairy, M. S. & Yeh, J. J. Photon statistics in multiphoton absorption and emission processes. *Phys. Rev. A* **21,** 1624–1631 (1980).
35. Glauber, R. J. The quantum theory of optical coherence. *Phys. Rev.* **130,** 2529–2539 (1963).
36. Kavokin, A., Baumberg, J. J., Malpuech, G. & Laussy, F. P. *Microcavities* (Oxford Univ. Press, 2011).
37. Kubanek, A. *et al.* Two-photon gateway in one-atom cavity quantum electrodynamics. *Phys. Rev. Lett.* **101,** 203602 (2008).
38. Hong, H.-G., Nha, H., Lee, J.-H. & An, K. Rigorous criterion for characterizing correlated multiphoton emissions. *Opt. Express* **18,** 7092–7100 (2010).
39. Plenio, M. B. & Knight, P. L. The quantum-jump approach to dissipative dynamics in quantum optics. *Rev. Mod. Phys.* **70,** 101–144 (1998).
40. Wiersig, J. *et al.* Direct observation of correlations between individual photon emission events of a microcavity laser. *Nature* **460,** 245–249 (2009).
41. Srinivas, M. D. & Davies, E. B. Photon counting probabilities in quantum optics. *Opt. Acta* **28,** 981–996 (1981).
42. Zoller, P., Marte, M. & Walls, D. F. Quantum jumps in atomic systems. *Phys. Rev. A* **35,** 198–207 (1987).
43. Osad'ko, I. S. Photon distribution functions of fluorescence photons from single nanoparticles: three different photon counting methods. *Opt. Spectrosc.* **107,** 948–958 (2009).
44. Carmichael, H. *An Open Systems Approach to Quantum Optics* Ch. 6, 110 (Springer, 1993).
45. Loudon, R. *The Quantum Theory of Light* (Oxford Science Publications, 2000).
46. Ota, Y., Iwamoto, S., Kumagai, N. & Arakawa, Y. Spontaneous two-photon emission from a single quantum dot. *Phys. Rev. Lett.* **107,** 233602 (2011).
47. Laucht, A. *et al.* Electrical control of spontaneous emission and strong coupling for a single quantum dot. *New J. Phys.* **11,** 023034 (2009).
48. Nissen, F., Fink, J. M., Mlynek, J. A., Wallraff, A. & Keeling, J. Collective suppression of linewidths in circuit QED. *Phys. Rev. Lett.* **110,** 203602 (2013).
49. Del Valle, E. Distilling one, two and entangled pairs of photons from a quantum dot with cavity QED effects and spectral filtering. *New J. Phys.* **15,** 025019 (2013).
50. Boitier, F., Godard, A., Rosencher, E. & Fabre, C. Measuring photon bunching at ultrashort timescale by two-photon absorption in semiconductors. *Nature Phys.* **5,** 267–270 (2009).

Acknowledgements

The authors thank J. Sánchez Wolff for assistance with Fig. 1. This work was supported by the POLAFLOW European Research Council starting grant, the Marie-Curie project Sensing Quantum Information Correlations and the Spanish Ministerio de Economía y Competitividad (MAT2011-22997). C.S.M. acknowledges a Formación de Personal Investigador grant. A.G.T and K.M. acknowledge support from the Alexander Von Humboldt Foundation and F.P.L. acknowledges support from a Ramón y Cajal contract.

Author contributions

F.P.L. and E.d.V. proposed the idea. C.S.M., E.d.V. and F.P.L. developed the theoretical formalism and the conceptual tools. C.S.M. implemented the theoretical methods and analysed the data. A.G.T., K.M., S.L., M.K. and J.J.F. contributed material, analysis tools and expertise. F.P.L., C.S.M., E.d.V., C.T. and J.J.F. wrote the main paper. C.S.M., E.d.V., A.G.T. and F.P.L. wrote the Supplementary Information. F.P.L. supervised the research. All authors discussed the results and its implications and commented on the manuscript.

Additional information

Supplementary information is available in the online version of the paper. Reprints and permissions information is available online at www.nature.com/reprints. Correspondence and requests for materials should be addressed to F.P.L.

Competing financial interests

The authors declare no competing financial interests.